Distributed Methodology for Reactive Power Support of Transmission System

Georgios C. Kryonidis
School of Electr. & Comput. Eng.
Aristotle University of Thessaloniki
Thessaloniki, Greece
kryonidi@ece.auth.gr

Maria E. Tsampouri
School of Electr. & Comput. Eng.
Aristotle University of Thessaloniki
Thessaloniki, Greece
tsamp.m@gmail.com

Kyriaki-Nefeli D. Malamaki
School of Electr. & Comput. Eng.
Aristotle University of Thessaloniki
Thessaloniki, Greece
kyriaki_nefeli@hotmail.com

Charis S. Demoulias
School of Electr. & Comput. Eng.
Aristotle University of Thessaloniki
Thessaloniki, Greece
chdimoul@auth.gr

2021 International Conference on Smart Energy Systems and Technologies (SEST) | 978-1-7281-7660-4/21/$31.00 ©2021 IEEE | DOI: 10.1109/SEST50973.2021.9543187

***Abstract*—This paper deals with the provision of reactive power support from distribution grids to the transmission system. To this end, a new distributed control scheme is proposed that coordinates the reactive power output of distributed generation (DG) units to meet a predefined reactive power set-point at the point of interconnection of the distribution grid with the transmission system. The coordination process is implemented in an optimal way minimizing the reactive power of DG units, while also satisfying the technical limits of the distribution grid. Time-series simulations on the IEEE 33-bus network are performed to evaluate the performance of the proposed method against existing solutions.**

***Index Terms*—Distributed algorithm, distributed generation, loss reduction, reactive power support, voltage control.**

I. Introduction

Traditionally, distribution grids were treated by the transmission system operators (TSOs) as passive elements without being actively involved in the control process. Nevertheless, the advent of distributed generation (DG) brought new control and monitoring functionalities, enabling their active participation at the transmission system operation [1]. This is also reflected in the demand connection code published by ENTSO-E, which introduces a closer cooperation between distribution system operators (DSOs) and TSOs to tackle new operational challenges raised by the gradual replacement of large-scale power plants with DG units [2].

Focusing on the provision of reactive power support (RPS), the authors in [3] demonstrated that the available reactive power of DG units can be used instead of the conventional compensation devices to effectively regulate the reactive power at the TSO-DSO interface. Furthermore, the performance of the well-established $Q(V)$ and $Q(P)$ droop control schemes is investigated in [4] and [5], respectively, in terms of providing RPS. Nevertheless, a decentralized implementation is assumed for these methods, where control actions are individually performed by each DG unit based only on local measurements. As a result, the reactive power at the TSO-DSO interface cannot be accurately controlled, since DG units operate in an uncoordinated way.

To overcome this limitation, a central controller is introduced in [6] to coordinate the decentralized operation of DG units equipped with $Q(V)$ droop control. The concept of the central controller is also adopted in [7], which is used to adjust the operating set-points of the DG units to meet a predefined power exchange at the TSO-DSO interface. In [8], a model-free coordination scheme is proposed to transform the distribution feeder into a controllable PV bus. More specifically, the reactive power of the distribution grid is automatically adjusted to regulate the voltage at the transmission system. Although the above-mentioned methods can effectively provide RPS to the transmission system, their impact on the performance of the distribution grid is not considered.

This drawback can be addressed by developing control strategies with integrated optimization objectives. In particular, the authors in [9] and [10] propose centralized, optimization-based methods for the provision of RPS. However, a linearized network model is assumed which may introduce inaccuracies and infeasible operating points during the real-time grid operation. The full nonlinear network model is considered in the optimization-based methods proposed in [11]–[13]. Scope of these methods is to regulate the reactive power exchange at the TSO-DSO interface with minimum network losses, while also satisfying the technical limits of the distribution grid. Nevertheless, centralized methods suffer from single-point failures due to the use of a central controller. Additionally, these methods use generation and consumption forecasts to determine the operating set-points of DG units. Thus, in case of forecast errors, miscalculations may occur leading to suboptimal and infeasible solutions. Finally, a complete knowledge of the network parameters and operating conditions is needed, limiting their applicability under real-field conditions.

In this paper, a new distributed control scheme is proposed for the provision of RPS at the TSO-DSO interface. Scope of the proposed method is to optimally coordinate the reactive power output of DG units to achieve a predefined RPS set-point without violating the technical constraints of the distribution grid. The optimization process targets at minimizing the reactive power used by the DG units. The distinct feature of the proposed method lies on the use of a data-driven distributed control architecture, avoiding the use of forecasts and the adverse effects caused by single-point failures. Furthermore, contrary to the centralized methods, the proposed approach requires limited information, thus allowing its implementation under real-field conditions.

II. Problem Formulation

The optimal provision of RPS at the TSO-DSO interface constitutes an optimization problem that is mathematically formulated using (1)-(9). More specifically, (1) is introduced as the objective function aiming to minimize the overall reactive power used by the DG units. As a result, the overall cost for implementing the RPS at the TSO-DSO interface is kept as minimum as possible.

$$\min \sum_{i \in N} |Q_{\mathrm{g},i}| \tag{1}$$

Here, $Q_{\mathrm{g},i}$ is the main control variable denoting the reactive power used by the DG unit located at node i, while N is the set of the network nodes. It is worth mentioning that a positive value of $Q_{\mathrm{g},i}$ indicates a leading power factor, i.e., the DG unit operates in overexcited mode producing reactive power. The model of the distribution grid is included in the optimization problem using (2) and (3) that represent the active and reactive power flowing through the network branches.

$$P_{ij} = V_i V_j [G_{ij} \cos(\theta_i - \theta_j) + B_{ij} \sin(\theta_i - \theta_j)] \tag{2}$$

$$Q_{ij} = V_i V_j [G_{ij} \sin(\theta_i - \theta_j) - B_{ij} \cos(\theta_i - \theta_j)] \tag{3}$$

P_{ij} and Q_{ij} are the active and reactive power flowing from node i to the directly connected node j. Furthermore, V_i and θ_i denote the magnitude and angle of the voltage at node i. Finally, G_{ij} and B_{ij} are the real and imaginary part of the ij-th element of the positive-sequence network admittance matrix.

The concept of the slack bus is introduced to model the transmission system. In particular, the transmission system is modeled as an ideal voltage source where the voltage angle is zero while the voltage magnitude (V_s) is calculated as follows:

$$V_s = V_{\mathrm{hv}} / [m(1 + \beta tap)] \tag{4}$$

where V_{hv} stands for the voltage magnitude of the HV network, tap denotes the tap position, β is the variation of the transformation ratio, and m is the nominal transformation ratio. Eq. (4) is introduced to model the on-load tap changer (OLTC) operation of the high-/medium-voltage (HV/MV) transformer.

The provision of RPS at the TSO-DSO interface is incorporated in the optimization problem by adding the following equality constraint:

$$Q_{\mathrm{set}} = \sum_{j \in N} Q_{sj} \tag{5}$$

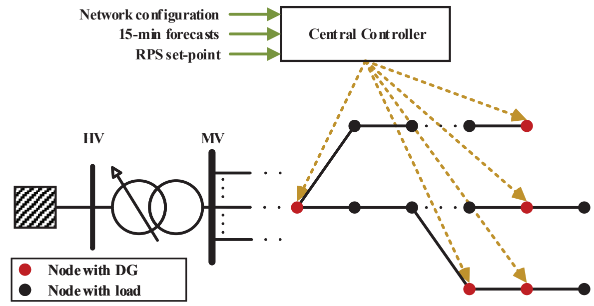

Fig. 1. Conceptual design of the centralized control scheme.

where Q_{set} is the reference value and Q_{sj} is the reactive power flowing from the slack bus (s) to the directly connected node j. Moreover, the active (P_i) and reactive power (Q_i) injections at node i are calculated according to

$$P_i = \sum_{j \in N} P_{ij} = P_{\mathrm{g},i} - P_{\mathrm{c},i} \tag{6}$$

$$Q_i = \sum_{j \in N} Q_{ij} = Q_{\mathrm{g},i} - Q_{\mathrm{c},i}. \tag{7}$$

Here, $P_{\mathrm{c},i}$ and $Q_{\mathrm{c},i}$ are the active and reactive power of the load connected to node i, respectively, whereas $P_{\mathrm{g},i}$ stands for the active power of the DG unit located at node i. Finally, (8) and (9) are used to model the reactive power capability of DG units and the technical constraints of the distribution grid, respectively.

$$Q_{\mathrm{min},i} \leq Q_{\mathrm{g},i} \leq Q_{\mathrm{max},i} \tag{8}$$

$$V_{\mathrm{min}} \leq V_i \leq V_{\mathrm{max}} \tag{9}$$

$Q_{\mathrm{min},i}$ and $Q_{\mathrm{max},i}$ are the minimum and maximum reactive power limits of the DG unit connected to node i, which are calculated following the procedure described in [14]. In case no DG unit is connected at node i, the corresponding reactive power limits are set equal to zero. Finally, V_{max} and V_{min} are the maximum and minimum permissible voltage limits.

III. Centralized Control Scheme

The optimal RPS provision at the TSO-DSO interface can be implemented by adopting the centralized approach depicted in Fig. 1. More specifically, a central controller is applied to solve the optimization problem of (1)-(9) using the following input data: (a) network configuration, (b) short-term generation and consumption forecasts, and (c) Q_{set}. The output data are the reactive power set-points which are forwarded to the DG units via an ICT infrastructure. This process is repeated at a regular basis, e.g., every 15 min. It is worth mentioning that between two consecutive solutions of the optimization problem, the reactive power output of each DG unit remains constant and equal to the last acquired value. As a result, in case of forecast errors, inaccuracies may occur, increasing also the possibility of voltage violations. Furthermore, the optimization problem of (1)-(9) requires a complete knowledge of the network parameters and operating conditions at each time instant, while single-point failures, e.g. central controller failure, cannot be effectively addressed.

IV. Proposed Method

Scope of the proposed method is to present a distributed way of updating the reactive power of each DG unit, achieving also near optimal solution. To facilitate the derivation of the update process, the mathematical formulation of the optimization problem is modified as follows:

$$\min \sum_{i \in N} Q_{\mathrm{g},i}^2 \tag{10}$$

s.t.

$$V_j^2 = V_i^2 + 2\left(R_{ij} P_{ij} + X_{ij} Q_{ij}\right) \tag{11}$$

$$P_{ij} = \sum_{k \in N_j^{\mathrm{d}}} P_{jk} + P_{\mathrm{g},j} - P_{\mathrm{c},j} \tag{12}$$

$$Q_{ij} = \sum_{k \in N_j^{\mathrm{d}}} Q_{jk} + Q_{\mathrm{g},j} - Q_{\mathrm{c},j} \tag{13}$$

$$V_s = V_{\mathrm{hv}} / [m(1 + \beta tap)] \tag{14}$$

$$Q_{\mathrm{set}} = Q_{\mathrm{TD}} = \sum_{j \in N} Q_{sj} \tag{15}$$

$$Q_{\mathrm{min},i} \leq Q_{\mathrm{g},i} \leq Q_{\mathrm{max},i} \tag{16}$$

$$V_{\mathrm{min}}^2 \leq V_i^2 \leq V_{\mathrm{max}}^2 \tag{17}$$

where N_j^d is the set of nodes located downstream of node j, while Q_{TD} is the reactive power flowing at the TSO-DSO interface. Eq. (10) is used instead of (1) as the objective function to accommodate the Lagrangian formulation presented below. Note that both approaches focus on the same objective, i.e., the minimization of the reactive power used by the DG units. Furthermore, (11)-(13) are the simplified DistFlow equations proposed in [15] that model the distribution grid. Due to the use of the square of the voltages in (11), (17) is used to limit the network voltages within the permissible limits.

The method of Lagrange multipliers is proposed to solve the optimization problem of (10)-(17) [16]. More specifically, the Lagrangian is calculated according to

$$\begin{aligned} L = &\sum_{i \in N} \lambda_i^u (V_i^2 - V_{\mathrm{max}}^2) + \sum_{i \in N} \lambda_i^l (-V_i^2 + V_{\mathrm{min}}^2) \\ &+ \sum_{i \in N} \mu_i^u (Q_{\mathrm{g},i} - Q_{\mathrm{max},i}) + \sum_{i \in N} \mu_i^l (-Q_{\mathrm{g},i} + Q_{\mathrm{min},i}) \\ &+ \nu (Q_{\mathrm{set}} - Q_{\mathrm{TD}}) + \sum_{i \in N} Q_{\mathrm{g},i}^2. \end{aligned} \tag{18}$$

Here, λ_i^u, λ_i^l, μ_i^u, and μ_i^l are the Lagrangian multipliers associated with the inequality constraints, i.e., (16) and (17), whereas ν is the Lagrangian multiplier related to the equality constraint as expressed by (15). It is worth mentioning that (11)-(13) are indirectly considered in the above Lagrangian via V_i^2. Moreover, (14) is excluded from the Lagrangian since tap is treated as an input parameter in the optimization problem determining the voltage at the slack bus (V_s).

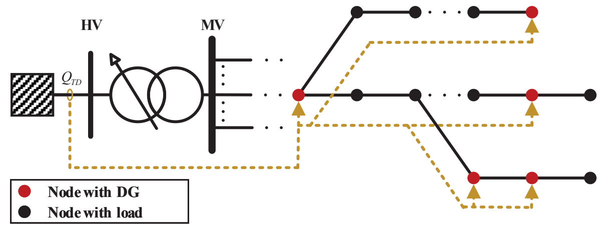

Fig. 2. Conceptual design of the distributed control scheme.

Substituting (11)-(13), and (15) to (18) and assuming $\frac{\partial L}{\partial Q_{\mathrm{g},i}} = 0$, (19) is obtained.

$$Q_{\mathrm{g,i}} = -\frac{1}{2}\left[\sum_{j \in N} \frac{\partial V_j^2}{\partial Q_{\mathrm{g,i}}} \left(\lambda_j^u - \lambda_j^l\right) + \left(\mu_i^u - \mu_i^l\right) - \nu\right] \tag{19}$$

The partial derivative in (19) can be directly calculated using (11). Nevertheless, to design a distributed update process with reduced communication needs only the partial derivative of the square voltage at node i with respect to the reactive power variation at the same node is considered. As a result, the reactive power of DG unit located at node i ($Q_{\mathrm{g,i}}(\tau+1)$) is updated as follows:

$$\begin{aligned} Q_{\mathrm{g,i}}(\tau+1) = -\frac{1}{2}\big[&X_{ii}\left(\lambda_i^u(\tau+1) - \lambda_i^l(\tau+1)\right) \\ &+ \left(\mu_i^u(\tau+1) - \mu_i^l(\tau+1)\right) - \nu(\tau+1)\big] \end{aligned} \tag{20}$$

where X_{ii} is the sum of the reactances of the lines that connect slack bus with node i. Furthermore, the updates of the Lagrangian multipliers are determined using (21).

$$\begin{aligned} \lambda_i^u(\tau+1) &= \left[\lambda_i^u(\tau) + \gamma(V_i^2 - V_{\mathrm{max}}^2)\right]_+ \\ \lambda_i^l(\tau+1) &= \left[\lambda_i^l(\tau) + \gamma(-V_i^2 + V_{\mathrm{min}}^2)\right]_+ \\ \mu_i^u(\tau+1) &= \left[\mu_i^u(\tau) + \delta(Q_{\mathrm{g},i} - Q_{\mathrm{max},i})\right]_+ \\ \mu_i^l(\tau+1) &= \left[\mu_i^l(\tau) + \delta(-Q_{\mathrm{g},i} + Q_{\mathrm{min},i})\right]_+ \\ \nu(\tau+1) &= \nu(\tau) + \epsilon(Q_{\mathrm{set}} - Q_{\mathrm{TD}}) \end{aligned} \tag{21}$$

Here, the operator $[\ ]_+$ defines the projection on the positive orthant, whereas γ, δ, and ϵ are positive constant parameters determining the convergence rate. These parameters are case-sensitive depending mainly on the configuration of the examined network and the number of DG units. In this paper, γ and δ are equal to 10^{-3}, while ϵ is equal to $2 \cdot 10^{-3}$.

The proposed control scheme can be implemented under real-field conditions by adopting the configuration presented in Fig. 2. In particular, an ICT infrastructure is used to forward Q_{TD} to the DG units. It is worth mentioning that a synchronous implementation is considered, i.e., the information is provided at the same time in the DG units. Afterward, each DG unit updates locally the Lagrangian multipliers according to (21) by combining local information, i.e., the voltage at the point of interconnection with grid, and information received by the ICT infrastructure, i.e., Q_{TD}. Finally, the updated reactive power output of each DG unit is calculated using (20).

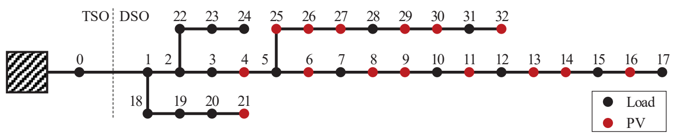

Fig. 3. Topology of the examined MV network [17].

TABLE I
RATED ACTIVE POWER OF PV UNITS

Node	MWp	Node	MWp	Node	MWp
4	0.35	6	0.50	8	0.70
9	0.30	11	0.80	13	0.35
14	0.70	16	0.50	21	0.50
25	0.25	26	0.70	27	0.25
29	0.80	30	0.35	32	0.35

V. NUMERICAL RESULTS

The performance of the proposed distributed methodology is evaluated by performing time-series simulations on the 12.66 kV MV distribution grid depicted in Fig. 3. Details regarding the network configuration, the line parameters, and the rated power of the loads are presented in [17]. Moreover, 15 PV units are connected to the nodes denoted with red color in Fig. 3 transforming the initially passive grid to active. The nominal power factor of the PV units is equal to 0.8, while their connection node and the corresponding rated power are presented in Table I. Finally, the voltage at the slack bus is kept constant and equal to 12.66 kV, while the minimum and maximum voltage limits are 0.95 and 1.05 p.u, respectively.

The simulation period is one day with a time resolution of 1 min. Normalized generation and consumption profiles, similar to those presented in Fig. 4 are arbitrary distributed to the PV units and loads. It is worth mentioning that the power factor of all loads remains constant and equal to the nominal value defined in [17]. The proposed method is compared against a centralized, optimization-based method. More specifically, the following scenarios are considered:

- Centralized method without RPS (CN). In this scenario, an optimization-based method is considered where the provision of RPS is neglected. Eqs. (1)-(4) and (6)-(9) are solved at each time instant using the IPOPT solver in GAMS [18].
- Proposed method without RPS (PN). Similar to CN, RPS is deactivated, i.e., $\nu = 0$. In this scenario, two softwares are employed, namely OpenDSS and MATLAB. The former is used as a power flow solver and the latter is employed to implement the iterative process as expressed by (20) and (21) at each time instant. Note that at each iteration, a connection is established between MATLAB and OpenDSS exchanging information, i.e., reactive power set-points and network voltages.
- Centralized method with RPS (CW). This is an enhanced version of the CN including also the provision of RPS. In particular, (1)-(9) are solved at each time instant using the IPOPT solver in GAMS [18].

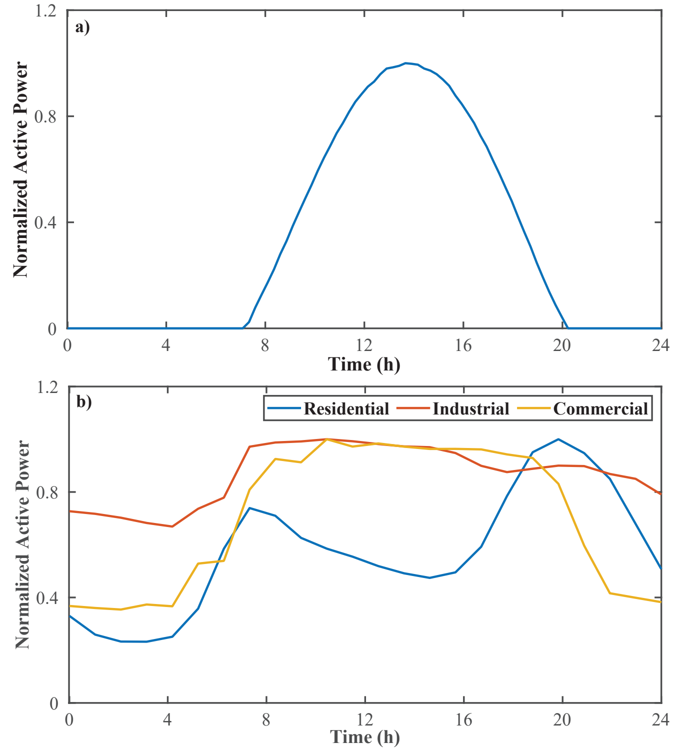

Fig. 4. Daily normalized active power profiles. a) Generation and b) consumption.

- Proposed method with RPS (PW). This is the complete version of the proposed methodology, considering also the provision of RPS.

The daily profile of the active and reactive power at the TSO-DSO interface is depicted in Fig. 5, while daily profiles associated with the operating conditions within the distribution grid are presented in Fig 6. In particular, the voltage magnitude at the most remote PV node, i.e., node 16, is illustrated in Fig. 6a. This is the most critical node for overvoltage mitigation since it presents the maximum network voltage in case no control is applied and PV units operate with unity power factor. The overall reactive power used by the PV units is shown in Fig. 6b. Furthermore, the network losses are presented in Fig. 6c. Finally, the daily reactive energy used by the PV units and the network energy losses are presented in Table II.

According to Fig. 5a, it can be observed that the distribution grid presents an inductive behaviour for all the simulation period in case RPS is neglected. On the contrary, the provision of the RPS actively controls the reactive power at the TSO-DSO interface reaching zero values, i.e., unity power factor. It worth mentioning that both CW and PW can effectively track the reference value at the TSO-DSO interface.

Considering the active power at the TSO-DSO interface, all the examined scenarios lead to a similar profile, as shown in Fig. 5b. Small mismatches are observed for specific time instants which are mainly related to the fact that each examined scenario leads to a different profile of network losses, as verified in Fig. 6c.

Focusing on the operating conditions within the distribution

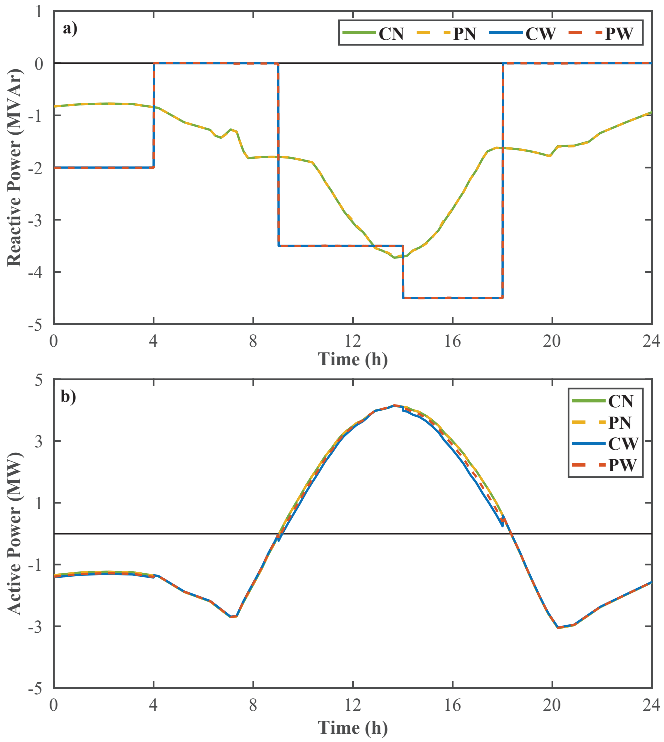

Fig. 5. Daily power profiles at TSO-DSO interface. a) Reactive power and b) active power. Positive sign indicates power flow from MV grid towards the upstream HV grid.

TABLE II
DAILY PV REACTIVE ENERGY AND NETWORK ENERGY LOSSES

	CN	PN	CW	PW
Energy (MVArh)	6.79	6.75	37.06	37.73
Losses (MWh)	4.02	3.99	5.75	4.88

grid, it can be concluded that all the examined scenarios can maintain the network voltages within the permissible limits, as shown in Fig. 6a. In case RPS is neglected, the voltage profile of CN and PN overlap. On the other hand, PW leads to a different voltage profile compared to the CW. Additionally, in both implementations, i.e. with and without RPS, the proposed control scheme leads to similar amounts of reactive power compared to the centralized method. This is also evident in Table II where the maximum mismatch is 1.81 %, indicating that the proposed control scheme can achieve near optimal solutions.

In terms of network losses, the proposed method leads to a reduced power profile compared to the centralized control scheme, as shown in Fig. 6c. Additionally, a reduction of 15.13 % is achieved in the daily network losses by the proposed method, as verified in Fig. 6c and Table II, revealing its superior performance against the centralized solution.

To assess the impact of forecast errors on the performance of the centralized, optimization-based solutions, a new series of time-series simulations are performed. This is attained by adopting the following procedure: Initially, the output data of the optimization process, i.e., the reactive power of PV units, are determined every 15 min assuming generation and consumption forecasts. Afterward, the output data are used to

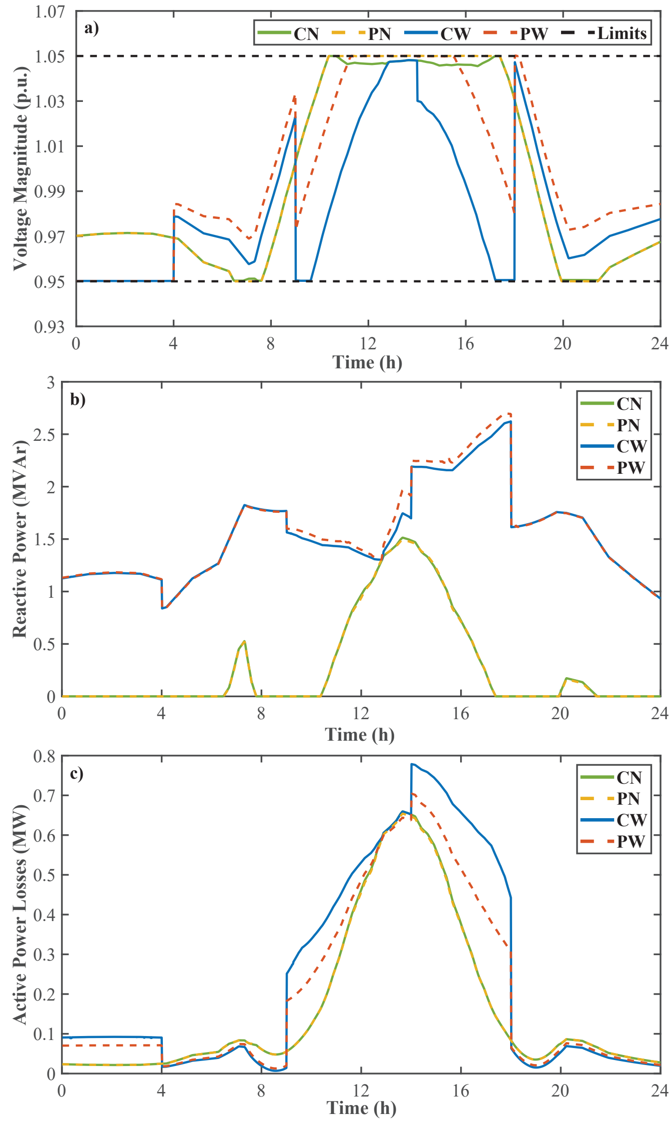

Fig. 6. Daily profiles associated with the distribution grid. a) Voltage magnitude at node 16, b) overall reactive power of PV units, and c) network losses.

perform a power flow analysis for a 15 min timeslot. During this analysis, forecasts errors are applied to the generation and consumption forecasts, varying from 5% to 30%. In this paper, forecast errors are only applied to consumption profiles, since the assumed PV profile is a sunny day that can be accurately predicted. The corresponding results are presented in Fig. 7. It can be observed that the centralized, optimization-based method fails to accurately control the reactive power at the TSO-DSO interface. Additionally, under-/overvoltages occur at the distribution grid, as shown in Fig. 7b. On the contrary, the performance of the proposed method is not affected by the assumed consumption and generation profiles, since it is a data-driven method. As a result, it can effectively control the reactive power at the TSO-DSO interface and ensure that network voltages are kept within the permissible limits.

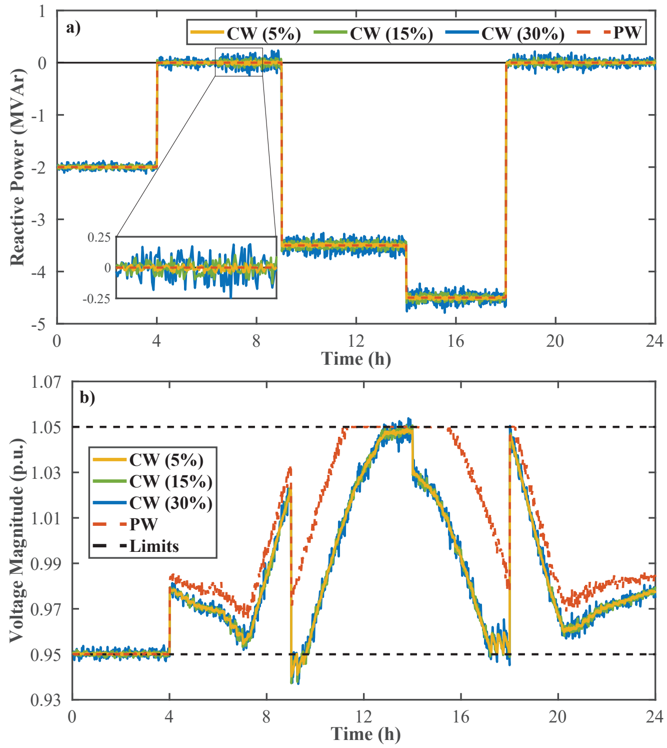

Fig. 7. Impact of forecast errors on the daily profiles. a) Reactive power at TSO-DSO interface and b) voltage magnitude at node 16.

VI. Conclusions and Future Work

In this paper, a new data-driven distributed control scheme is proposed for the provision of RPS at the TSO-DSO interface. The proposed method coordinates the reactive power of DG units to achieve a predefined RPS set-point, considering also the technical constraints of the distribution grid. The validity of the proposed method is demonstrated by performing time-series simulations on a MV distribution grid, highlighting its improved performance compared to centralized methods in terms of robustness to forecast errors. Furthermore, the proposed method leads to near optimal solutions.

Future work will be carried out to add new objectives in the developed control scheme, e.g., minimization of the network losses. Additionally, the asychronous information exchange among the neighbouring DG units will be investigated. Further, new control variables will be considered and integrated in the proposed method such as the active and reactive power of converter-interfaced battery energy storage systems, capacitor banks and shunt reactors at HV/MV substation, etc. Finally, a new cooperation scheme will be developed to combine the developed distributed method with the OLTC operation of the HV/MV transformer.

Acknowledgment

This research is co-financed by Greece and the European Union (European Social Fund - ESF) through the Operational Programme "Human Resource Development, Education and Lifelong Learning" in the context of the project "Reinforcement of Postdoctoral Researchers - 2nd Cycle" (MIS-5033021), implemented by the State Scholarships Foundation (IKY).

References

[1] S. Karagiannopoulos, J. Gallmann, M. G. Vayá, P. Aristidou, and G. Hug, "Active distribution grids offering ancillary services in islanded and grid-connected mode," *IEEE Trans. Smart Grid*, vol. 11, no. 1, pp. 623–633, 2020.

[2] ENTSO-E, "Demand connection code," *Official J. Eur. Union*, Aug. 2016.

[3] M. Kraiczy, H. Wang, S. Schmidt, F. Wirtz, and M. Braun, "Reactive power management at the transmission–distribution interface with the support of distributed generators – a grid planning approach," *IET Gener., Transm. Distrib.*, vol. 12, no. 22, pp. 5949–5955, 2018.

[4] Z. Cheng and X. Feng, "A study of DER Volt and Var droop aggregation for reactive power support to transmission system," in *2018 IEEE Power Energy Soc. General Meeting (PESGM)*, 2018, pp. 1–5.

[5] M. Tomaszewski, S. Stanković, I. Leisse, and L. Söder, "Minimization of reactive power exchange at the DSO/TSO interface: Öland case," in *2019 IEEE PES Innov. Smart Grid Technol. Europe (ISGT-Europe)*, 2019, pp. 1–5.

[6] G. Valverde, D. Shchetinin, and G. Hug-Glanzmann, "Coordination of distributed reactive power sources for voltage support of transmission networks," *IEEE Trans. Sustain. Energy*, vol. 10, no. 3, pp. 1544–1553, 2019.

[7] D. M. Gonzalez, L. Robitzky, S. Liemann, U. Häger, J. Myrzik, and C. Rehtanz, "Distribution network control scheme for power flow regulation at the interconnection point between transmission and distribution system," in *2016 IEEE Innov. Smart Grid Technol. - Asia (ISGT-Asia)*, 2016, pp. 23–28.

[8] D. B. Arnold, M. D. Sankur, M. Negrete-Pincetic, and D. S. Callaway, "Model-free optimal coordination of distributed energy resources for provisioning transmission-level services," *IEEE Trans. Power Syst.*, vol. 33, no. 1, pp. 817–828, 2018.

[9] G. Valverde and T. Van Cutsem, "Control of dispersed generation to regulate distribution and support transmission voltages," in *2013 IEEE Grenoble Conf.*, 2013, pp. 1–6.

[10] J. Morin, F. Colas, S. Grenard, J. Dieulot, and X. Guillaud, "Coordinated predictive control in active distribution networks with HV/MV reactive power constraint," in *2016 IEEE PES Innov. Smart Grid Technol. Conf. Europe (ISGT-Europe)*, 2016, pp. 1–6.

[11] K. Tang, R. Fang, L. Wang, J. Li, S. Dong, and Y. Song, "Reactive power provision for voltage support activating flexibility of active distribution networks via a TSO-DSO interactive mechanism," in *2019 IEEE Innov. Smart Grid Technol. - Asia (ISGT Asia)*, 2019, pp. 116–121.

[12] S. Karagiannopoulos, C. Mylonas, P. Aristidou, and G. Hug, "Active distribution grids providing voltage support: The Swiss case," *IEEE Trans. Smart Grid*, article in press.

[13] Y. Yi, X. Chu, and Y. Liu, "Activating reactive power support from active distribution systems," in *2018 IEEE Power Energy Soc. General Meeting (PESGM)*, 2018, pp. 1–5.

[14] G. C. Kryonidis, C. S. Demoulias, and G. K. Papagiannis, "A two-stage solution to the bi-objective optimal voltage regulation problem," *IEEE Trans. Sustain. Energy*, vol. 11, no. 2, pp. 928–937, 2020.

[15] M. Baran and F. F. Wu, "Optimal sizing of capacitors placed on a radial distribution system," *IEEE Trans. Power Del.*, vol. 4, no. 1, pp. 735–743, 1989.

[16] Z. Tang, D. J. Hill, and T. Liu, "Distributed coordinated reactive power control for voltage regulation in distribution networks," *IEEE Trans. Smart Grid*, vol. 12, no. 1, pp. 312–323, 2021.

[17] M. E. Baran and F. F. Wu, "Network reconfiguration in distribution systems for loss reduction and load balancing," *IEEE Trans. Power Del.*, vol. 4, no. 2, pp. 1401–1407, 1989.

[18] R. E. Rosenthal, *GAMS: A User's Guide*, GAMS Development Corporation, Washington, DC, USA, 2016.